s c c h
software competence center
hagenberg

FUZZY.LOGIC.LAB.LINZ

Advances in Knowledge-Based Technologies

Proceedings of the Master and PhD Seminar Summer term 2010, part 1

Softwarepark Hagenberg
SCCH, Room 0/2
7 and 8 April 2010

Software Competence Center Hagenberg
Softwarepark 21
A-4232 Hagenberg
Tel. +43 7236 3343 800
Fax +43 7236 3343 888
www.scch.at

Fuzzy Logic Laboratorium Linz
Softwarepark 21
A-4232 Hagenberg
Tel. +43 7236 3343 431
Fax +43 7236 3343 434
www.flll.jku.at

Program

Session 1: Wednesday, 7 April, Chair: Bernhard Moser

15:00 Holger Schöner:
Time of Flight Camera Image Denoising Improvements

15:30 Jean-Luc Bouchot:
The Fast Discrepancy: Theory and Application

Session 2: Thursday, 8 April, Chair: Roland Richter

9:00 Bertran Steinsky:
Labyrinth Fractals

9:30 Bettina Heise:
Phase-based approaches in microscopy and OCT/CPM techniques

10:00 Verena Schlager:
Coherence Microscopy 3D Image Processing

Session 3: Thursday, 8 April, Chair: Bernhard Moser

10:45 Edwin Lughofer:
On Dynamic Soft Dimension Reduction in Evolving Fuzzy Classifiers

11:15 Wolfgang Heidl:
Classifier-based analysis of visual inspection: Gender differences in decision-making

Image Processing for 3D-Scans Generated by TOF Range Cameras

Frank Bauer, Holger Schöner, Adrian Dorrington, Bettina Heise, Volkmar Wieser, Andrew Payne, Michael J. Cree and Bernhard Moser

Abstract

Time-of-flight (TOF) full-field range cameras use a correlative imaging technique to generate three-dimensional measurements of the environment. Though reliable and cheap they have the disadvantage of high measurement noise and errors that limit the practical use of these cameras in industrial applications.

We show how some of these limitations can be overcome with standard image processing techniques specially adapted to TOF camera data, which can be used to reduce the measurement noise. Three of these are compared on synthetic data and on data acquired from two different off-the-shelf TOF cameras. Best results are obtained with an adapted Anisotropic Diffusion technique.

1 Introduction

3D-object recognition is a task which is becoming increasingly important in real world applications such as industrial automation and surveillance. One promising technique for acquiring such data is full-field Time-of-Flight (TOF) range imaging. This technique uses active illumination and correlative image sensing to produce an image that contains both distance and intensity information in every pixel.

As range imaging technology advances, affordable, compact, and reliable camera systems are becoming available. However, measurements from these cameras still suffer from high noise levels and undesirable measurement artefacts, which often prohibit their use in many applications. By applying state of the art image processing to range image data, we obtain information more suitable for automatic post- processing and object recognition.

In our presentation we review the different kinds of noise and artefacts commonly seen in range images and present denoising techniques especially adapted for these situations. These techniques are applied to data acquired with two different commercially available TOF range cameras, showing significant improvements in image quality.

2 Performance on Synthetic Data

For a systematic comparison of the aforementioned denoising methods we used synthetically generated images. The background is a simple plane with constant distance, possibly overlaid by a pattern of bumps of configurable amplitude, by adding a low frequency 2D sine wave. 5 further planes are then placed at random positions and in random distance with given variance before or behind the background. They are also overlaid by bumps of configurable size, and can have a random tilt (slope) of a given variance and random direction. This is to simulate more realistic non-planar object surfaces. The intensity of background is set to a relatively low level, while

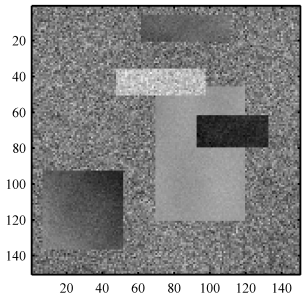

Figure 1: Example for a range image of a synthetic data example from scene "medium bumps/tilts."

Table 1: Performance (RMSE and Std.Dev. for 50 Realizations) of Denoising on Synthetic Data

Scene Characteristics	Averaging	EAD	Clustering	Wavlet	SNR [dB]
no bumps/tilts	0.52±0.061	0.12±0.033	**0.08±0.065**	0.22±0.037	0.11±4.070
medium bumps/tilts	0.54±0.061	**0.12±0.022**	0.18±0.077	0.24±0.034	2.05±3.066
medium bumps	0.54±0.076	**0.12±0.024**	**0.12±0.052**	0.24±0.052	1.83±2.686
strong bumps	0.54±0.074	**0.12±0.037**	0.21±0.069	0.24±0.045	2.02±2.781
medium tilts	0.54±0.064	**0.12±0.024**	0.19±0.115	0.24±0.036	1.76±3.294
strong tilts	0.54±0.070	**0.08±0.016**	0.39±0.159	0.26±0.037	4.67±2.455
very low noise	0.15±0.020	**0.03±0.005**	0.09±0.039	0.07±0.011	11.69±2.336
low noise	0.32±0.036	**0.05±0.009**	0.10±0.053	0.14±0.022	6.85±3.336
strong noise	0.78±0.097	**0.18±0.037**	**0.19±0.116**	0.33±0.047	-1.28±3.508
very strong noise	1.17±0.137	**0.28±0.041**	**0.26±0.164**	0.46±0.098	-4.66±3.219

that of the objects is chosen randomly, and noise is added to both range and to a lesser degree to intensity images. Variance of noise is scaled according to the inverse intensity of the respective pixel. We defined some test scenarios where we varied the presence and strength of bumps, of tilts, and the noise level. Fig. 1 shows an example for such a generated scene (range image), which medium bumps (only slightly visible because of the noise) and tilts of the object planes. Tab. 1 gives a short description for generated scenarios, the results for each denoising algorithm (measured as the root mean squared error RMSE between the denoised and the original images), and the average Signal to Noise ratio (SNR), together with standard deviation. These results were obtained by first optimizing the parameters of each algorithm for five random realizations of the corresponding scenario, and then applying the method with fixed parameters to 50 other random realizations of that scenario (the standard deviations are taken from these test samples). The averaging (and other denoising methods) had four range and intensity images with independent noise (for each time point and pixel) from each scene realization available. The best performing method is printed in bold; statistical significance of performance difference was tested pairwise between algorithms using matched pairs Wilcoxon signed-ranks test (1) with a significance level of 0.05, with Bonferroni correction to account for multiple testing.

It was found, that for such scenes with widely varying levels of noise and other image characteristics, the EAD method overall performed best. It significantly outperforms the other methods, or is among the best for all but one of the considered scene variants. The Clustering approach also performs well, as long as the scene does not contain strong slopes. The EAD and wavelet methods are relatively robust, while the clustering approach has a higher variation in denoising quality.

Acknowledgment

The authors from FLLL gratefully acknowledge the financial support by the Upper Austrian Technology and Research Promotion. The SCCH gratefully acknowledges funding of part of this work by the Austrian COMET program.

References

[1] D. Sheskin, *Parametric and Nonparametric Statistical Procedures*. Chapman&Hall/CRC, 2004.

The Fast Discrepancy: Theory and Application

Jean-Luc Bouchot

Johannes Kepler University Linz
FLLL-Hagenberg, Software Competence Center Hagenberg,
A-4232 Hagenberg, Austria
jean-luc.bouchot@jku.at

Abstract. With this introduction we aim to present a new approach to Hermann Weyl's concept of discrepancy. Indeed as shown in many articles (see [Mos09] or [NW87] for example) the discrepancy norm seems to be a perfect concept to be used as a correlation measure. However, even if it has shown good results, the discrepancy norm is much slower than its competitors such as the cross correlation approach. This is way we introduce an approximation based on L_p-norms which is much faster to compute. It is shown that this approximation have similar behavior as the discrepancy norm but is much more competitive with known approaches.

1 Introduction

As the discrepancy norm as shown really good results, we want to introduce a novel approach to Hermann Weyl's concept which will be faster and will show similar results. A first study on a 1-dimensional case can be found in [BHM10]. In this paper we want to introduce all good formulas that will be useful for further analysis. That means that after recalling the definition of the discrepancy norm (in section 2) we will introduce the fast approximation, and show some properties (section 3). In next section (4) we introduce an autocorrelation concept based on the discrepancy norm for an application in financial domain. Finally, in the last section we give an idea of what could be the next steps for the discrepancy norm and its approximations.

2 Hermann Weyl's Discrepancy Measure

For a summable sequence of real values $f = (f_i)_{i\in\mathbb{Z}}$, $\sum_{i\in\mathbb{Z}} |f_i| < \infty$, Weyl's discrepancy concept, see [Wey16], leads to the definition

$$\|f\|_D := \sup\left\{ \left| \sum_{i=n_1}^{n_2} f(i) \right| : n_1, n_2 \in \mathbb{Z} \right\}. \tag{1}$$

With this equation with have following properties:

– $\|.\|_D$ is a norm.

- $\|f\|_D = \max_k \sum_{i=0}^{k} f(i) - \min_k \sum_{i=0}^{k} f(i)$
- Let $\|f - f(.-t)\|_D$ is monotonically increasing with t getting bigger.

The equation 1 can be extended to multivariate variable using Cartesian products of intervals (see [Mos09] or [MH08] for more details). This leads to the following definition for the discrepancy norm for image:

$$\|f\|_D = \max_{\mathcal{I}_1,\mathcal{I}_2 \in \mathcal{I}(\mathbb{Z})} |\sum_{i\in\mathcal{I}_1}\sum_{j\in\mathcal{I}_2} f_{i,j}| \tag{2}$$

where $\mathcal{I}(\mathbb{Z})$ denotes the set of all intervals of $\mathbb{Z}$.

3 1D Approximation

In this section the discrepancy is norm is approximated by a formula that can be computed by convolution which reduces the computational complexity to $O(n\log(n))$ for n be the number of discrete support points. In this section we restrict to finite support intervals $\mathcal{I}$, $n = |\mathcal{I}| > 1$. For convenience without loss of generality, we restrict to intervals $\mathcal{I} = \{1, \dots, n\}$ starting at 1. Further on, for convenience let us set

$$F_k(f) := \sum_{i=0}^{k} f_i$$
$$\chi_p[f](k) := e^{p\sum_{i=0}^{k} f_i} = e^{pF_k(f)}$$

where by definition we set $f_0 = 0$. The t-mean M_t is defined by

$$M_t(f) = \left(\frac{1}{N+1}\sum_{i=0}^{N} |f_i|^t\right)^{\frac{1}{t}}$$

which for $t = +1$ yields the arithmetic and for $t = -1$ yields the harmonic mean. Then, let us define

$$\Gamma_p(f) = \frac{1}{p}\ln\left(\frac{M_{+1}(\chi_p[f])}{M_{-1}(\chi_p[f])}\right) \tag{3}$$

which is well defined due to the fact that the t-mean M_t is monotonically increasing with t and, that due to the construction of χ_p we have $0 < \min_{k\in\{0,\cdots,N\}} \chi_p[f](k) \leq M_{-1}(\chi_p[f]) \leq M_1(\chi_p[f])$. Though Γ_p can not be proven to satisfy all norm properties, we get similar and approximative results, see [BHM10] for more details.

- Γ_p is positive definite
- approximative homogeneity:
  $\Gamma_p(\lambda f) = |\lambda| \cdot \Gamma_{|\lambda| p}(f)$
- approximative triangular inequality:
  $\Gamma_p(f+g) \leq \Gamma_p(f) + \Gamma_p(g) + \frac{2}{p}\ln(n+1)$

Finally we state the main result of this section:

Theorem 1. *Γ_p approximates the discrepancy norm in the sense of*

$$\Gamma_p(f) \leq ||f||_D < \Gamma_p(f) + \frac{2}{p}\ln(n+1) \tag{4}$$

and can be computed by convolution

$$h = \frac{1}{p}\ln(F * G) + \frac{1}{p}\ln(F^{-1} * G^{-1}) \tag{5}$$

where $F = \chi_p[f]$, $G = \chi_{-p}[g]$.

4 Discrepancy-Based Autocorrelation

In this section a correlation coefficient based on the discrepancy norm is proposed. The construction imitates the classical Pearson's formula, which can be expressed by means of an inner product

$$\mathrm{corr}(f,g) = \frac{\langle f,g\rangle}{\|f\|\|g\|}.$$

For any inner product space with inner product $\langle .,.\rangle$ the parallelogram law can be derived $\|f-g\|^2+\|f+g\|^2 = 2(\|f\|^2+\|g\|^2)$, which together with $\|f+g\|^2 = \|f\|^2+\|g\|^2+2\langle f,g\rangle$, induces a representation of the inner product by means of the norm

$$\langle f,g\rangle = (\|f+g\|^2 - \|f-g\|^2)/4. \tag{6}$$

Note that the discrepancy norm does not fulfill the parallelogram law, consider, e.g., $f=(1,1,-1)$ and $g=(1,-1,1)$, then $\|f-g\|_D^2+\|f+g\|_D^2 = \|(2,0,0)\|_D^2+\|(0,2,2)\|_D^2 = 20 \neq 2(\|f\|_D^2+\|g\|_D^2) = 10$. Anyway, formula (5) yields a reasonable correlation coefficient for not vanishing $f,g \in F_{\mathcal{I}}$

$$\mathrm{corr}_D(f,g) := \frac{1}{4}\frac{\|f+g\|_D^2 - \|f-g\|_D^2}{\|f\|_D^2\|g\|_D^2} \in [-1,1]. \tag{7}$$

The range of $\mathrm{corr}_D(.,.) \in [-1,1]$ directly follows from the triangle inequality of the norm, so does $\mathrm{corr}_D(f,\lambda f) = 1$ for $\lambda \in \mathbb{R}\backslash\{0\}$.

Observe that for $f \geq 0$ we have $\|f\|_D = \|f\|_1 = \sum_f(i)$, therefore, for $g \geq f \geq 0$, $f \neq 0$ we obtain

$$\begin{aligned}\mathrm{corr}_D(f,g) &= \frac{(\sum_i f(i)+g(i))^2 - (f(i)-g(i))^2}{4\sum_f f(i)\sum_i g(i)}\\ &= 1.\end{aligned}$$

If we correlate f with itself for a nonnegative $f \geq 0$ note that

$$\begin{aligned}&\mathrm{corr}_D(f(.), f(.-t))\\ =\ &\frac{1}{4}\frac{\|f(.)+f(.-t)\|_D^2 - \|f(.)-f(.-t)\|_D^2}{\|f(.)\|_D^2+\|f(.-t)\|_D^2}\\ =\ &\frac{4\|f(.)\|_D^2 - \|f(.)-f(.-t)\|_D^2}{4\|f(.)\|_D^2}\end{aligned}$$

which means that, due to the monotonicity of the discrepancy norm of the difference of time-shifted non-negative functions as a function of the time-shift, the autocorrelation based on the discrepancy norm

$$\text{autocorr}_D[f](t) := \text{corr}_D(f(.), f(. - t)) \tag{8}$$

is monotonically decreasing for $t \geq 0$.

5 Outlook

As shown in this paper, the discrepancy concept has many advantages. Its approximation competes with the known method as the cross correlation or the Pearson coefficient in terms of time consumption whereas it shows similar results to the original discrepancy norm. Though more stuff has to be done. Indeed, it could be interesting to

- Use the approximation on 2D data,
- Calculate intraclass similarity (useful for textures or support vectors algorithm),
- Estimate its behavior in front of basic transformations.

References

[BHM10] J.L. Bouchot, J. Himmelbauer, and B. Moser. On autocorrelation based on Hermann Weyl's discrepancy norm for time series analysis. Technical Report SCCH-TR-1007, 2010. accepted for publication, WCCI2010.

[MH08] B. Moser and T. Hoch. Misalignment measure based on Hermann Weyl's discrepancy. In A. Kuijper, B. Heise, and L. Muresan, editors, *Proc. of 32nd Workshop of the Austrian Association for Pattern Recognition (AAPR/OAGM)*, volume 232, pages 187–197. Austrian Computer Society, 2008.

[Mos09] B. Moser. Similarity measure for image and volumetric data based on Hermann Weyl's discrepancy measure. *IEEE Transactions on Pattern Analysis and Machine Intelligence (TPAMI)*, 99:DOI 10.1109/TPAMI.2009.50, 2009. (Technical Report SCCH-TR-0813).

[NW87] H. Neunzert and B. Wetton. Pattern recognition using measure space metrics. Technical Report 28, Universität Kaiserslautern, Fachbereich Mathematik, November 1987.

[Wey16] H. Weyl. Über die Gleichverteilung von Zahlen mod. Eins. *Math. Ann.*, 77:313–352, 1916.

Labyrinth Fractals

Ligia Loreta Cristea
Technical University of Graz
Steyrergasse 30
8010 Graz
Austria
cristea@finanz.math.tu-graz.ac.at

Bertran Steinsky
Johannes Kepler University Linz
Department of Knowledge-Based Mathematical Systems
Austria
bertran.steinsky@jku.at *

April 1, 2010

Keywords: fractal, infinite curve length, dendrite, tree

AMS Classification: 14Q05, 26B05, 28A75, 28A80, 51M25, 52A38

The talk will recapitulate the contents of two articles by Cristea and Steinsky[4, 5]. Cristea and Steinsky studied 4×4-labyrinth fractals[4], which are self similar dendrites, i.e., "treelike" structures, in the Euclidean plane and $m \times m$-labyrinth fractals[5], for $m \geq 5$.

For all 4×4-labyrinth fractals we answer the question, whether there is a curve of finite length in the fractal[6] from one point to another point in the fractal. There may be two cases. In the first case, between any two points in the fractal there is a unique arc a, the length of a is infinite, and the set of points, where no tangent exists to a, is dense in a. For a definition of an arc, we refer to Kuratowski[11]. In the second case, there are also pairs of points between that there is a unique arc of finite length. Labyrinth fractals are fractal sets obtained by an iterative construction and, additionally, have three properties, which we demand. An example for the first and the second step of the construction is given in Figure 1. It turns out that labyrinth fractals are dendrites, which yields that between any two points in a labyrinth fractal there is a unique arc in the

*This research was supported by the Austrian Science Fund (FWF), Project P20412-N18, at the Technical University of Graz, Institute for Mathematics A.

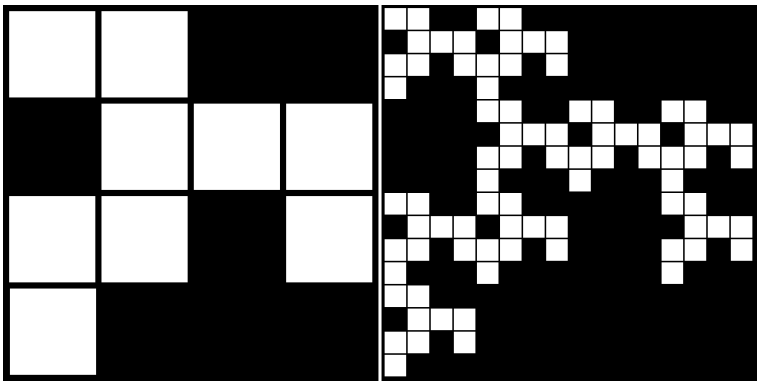

Figure 1: L_1 and L_2.

labyrinth fractal. We note that in the literature there are many examples of continuous curves with infinite length, like the von Koch curve([9],[10]), the Peano curve[13], the Hilbert curve[8], or the dragon curve [2, Example 5.1.6].

In a recent paper Cristea[3] introduced certain Moran fractals in the unit square, called limit net sets, and established several connectedness properties as connectivity, local connectivity, or arcwise connectivity. The construction of net sets is similar to that of labyrinth fractals, but net sets need not be self similar and the "black" squares are chosen to satisfy certain conditions which in a sense assure that they are "well distributed".

Whether the length of an arc between two points in a labyrinth fractal is infinite, depends on whether the labyrinth fractal is horizontally or vertically blocked, which means that there is no straight line connection from left to right or from top to bottom within the fractal. If the labyrinth fractal is horizontally *and* vertically blocked then the length of the arc between any two points in the labyrinth fractal is infinite. We note that in this case the box counting dimension of every such arc is greater than 1.

Also, for general $m \times m$-labyrinth fractals we showed that between any two points in the fractal there is a unique arc a, the length of a is infinite, and the set of points, where no tangent exists to a, is dense in a. Following Akiyama *et al.*[1, Remark 3.2] or Hata[7, Remark 2, p. 391], we may find more examples of curves with infinite length. But we note that not all of these curves have the property that the distance between any two points of the curve (seen as a set of points) is infinite, as it is the case for labyrinth fractals.

References

[1] S. Akiyama, J. M. Thuswaldner, *A survey on topological properties of tiles related to number systems*, Geom. Dedicata **109**, 89–105, 2004

[2] J.-P. Allouche and J. Shallit, *Automatic Sequences: Theory, Applications, Generalizations*, Cambridge, England: Cambridge University Press, pp. 155-156, 2003.

[3] L. L. Cristea, *On the connectedness of limit net sets*, Submitted 2008

[4] L. L. Cristea, B. Steinsky, *Curves of Infinite Length in* 4×4 *Labyrinth Fractals*, Geometriae Dedicata, **141**, 1–17, 2009

[5] L. L. Cristea, B. Steinsky, *Curves of Infinite Length in Labyrinth Fractals*, Proceedings of the Edinburgh Mathematical Society, to appear, 2010

[6] K. J. Falconer, *Fractal geometry, Mathematical Foundations and applications*, John Wiley & Sons, Chichester, 1990

[7] M. Hata, *On the structure of self-similar sets*, Japan J. Appl. Math. **2**, no. 2, 381–414, 1985

[8] D. Hilbert, *Über die stetige Abbildung einer Linie auf ein Flachenstück*, Math. Ann. **38**, 459–460, 1891.

[9] H. von Koch, *Sur une courbe continue sans tangente, obtenue par une construction géométrique élémentaire*, Archiv för Matemat. **1**, 681–702, 1904

[10] H. von Koch, *Une méthode géométrique élémentaire pour l'étude de certaines questions de la théorie des courbes planes*, Acta Math. **30**, 145–174, 1906

[11] K. Kuratowski, Topology, Volume II, Academic Press, New York and London, 1968

[12] P. A. P. Moran, *Additive functions of intervals and Hausdorff measure*, Proc. Cambridge Philos. Soc. **42** (1946), 15–23

[13] G. Peano, *Sur une courbe, qui remplit une aire plane.*, Math. Ann. *36*, 157-160, 1890

Phase-based approaches in Microscopy and Optical Coherence Tomography

Bettina Heise, FLLL, CDL MS-MACH, JKU LINZ

Abstract: Motivated from phase contrast microscopy as a well-known visualization technique, we have investigated, how phase sensitive imaging approaches in combination with quantitative analysis methods can be realized in field of Optical Coherence Tomography (OCT). OCT in its conventional configuration working on the principle of low coherence interferometry is exploiting the reflectance (i.e. intensity of the backscattered light) from micro- scattereres or interfaces to obtain structural information from inside the sample. But this imaging technique can also be modified to phase-sensitive versions. They are utilizing either the complex nature of light (i.e. the phase resp. phase differences as in case of Differential Phase Contrast OCT (DPC-OCT)) or from the complex representation of light wave derived quantities as polarization resulting in phase retardation signals (as in case of Polarization Sensitive OCT (PS-OCT)). We have shown how these configurations can be realized in an optical setup allowing 2D-based phase measurements (in particular differential phase 2D measurement configuration) and / or a 2D image analysis (in particular for phase retardation images by 2D fringe analysis in PS-OCT). The both 2D realizations are outperforming 1D configurations and approaches especially in case of low SNR DPC-OCT images or complicated fringe structures in PS-OCT imaging. They allow finally to obtain depth or spatially resolved information about embedded phase structures (in DPC-OCT) or about anisotropies, birefringence or stress resp. inherent in the investigated sample (in PS-OCT).

Coherence Microscopy 3D Image Processing

Outline Master Thesis

Verena Schlager
Johannes Kepler Universität Linz
FLLL / CDL-MS-MACH

April 08, 2010

Abstract

Optical coherence tomography (OCT), a technique originally proposed for applications in the field of biomedical diagnostics, is shown to be an efficient measurement technique for a multitude of problems posed in technical engineering and material research [1]. Coherence microscopy (CM) should bring us to a still more efficient technique for analyzing surfaces of organic or polymer material.
In my master thesis I want to get rid of the high amount of 3D data. Therefore I work with different (3D) image processing software like Matlab, MAVI or G'MIC. I analyse their assets and drawbacks and use their advantages for analyzing the CM images. I will especially cover denoising and segmentation of the images to get an accurate mathematical model of the sample structure. At the end there should be a good and fast three dimensional representation available to visualize and analyze the 3D CM images.
At this time I successfully tried out a wavelet denoising based on a gaussian noise model like in the RNA expression profiling in [2]. I achieved a good 3D visualization of the woven sample within an acceptable runtime.

References

[1] D. Stifter, K. Wiesauer, M. Wurm et.al., *Investigation of polymer and polymer/fibre composite materials with optical coherence tomography*, DD MMM 2007

[2] J. Hesse, J. Jacak, L. Muresan et.al., *RNA expression profiling at the single molecule level*, Genome Research 2006

On Dynamic Soft Dimension Reduction in Evolving Fuzzy Classifiers

Edwin Lughofer [a]

[a] *Johannes Kepler University Linz, Department of Knowledge-based Mathematical Systems, Altenbergerstrasse 69, A-4040 Linz, Austria, email: edwin.lughofer@jku.at*

Abstract

In this paper, we present an approach for addressing the problem of dynamic dimension reduction during on-line training, evolution and updating of evolving fuzzy classifiers (EFC). The basic idea of our approach is that, instead of permanently changing the list of most important features with newly loaded data blocks (which may cause abrupt changes in the input structure of the fuzzy classifiers), we generalize the concept of incremental feature selection to an incremental feature weighting approach: features are assigned weights in [0,1] according to their importance level. These weights are permanently updated during on-line mode and guarantee a smooth learning process in the evolving fuzzy classifiers, as they change softly and continuously over time. In some cases, when the weights become (approximately) 0, an automatic switching off of some features and therefore a (soft) dimension reduction is achieved. Two novel incremental feature weighting strategies are proposed in this paper, one based on a leave-one-out, the other based on a feature-wise separability criterion. We will describe the integration concept of the feature weights in the evolving fuzzy classifiers, using single and multi-model architecture, where *FLEXFIS-Class SM* and *FLEXFIS-Class MM* serve as training engines. The whole approach of integrated incremental feature weighting in evolving fuzzy classifiers will be evaluated based on high-dimensional on-line real-world classification scenarios and based on data from the Internet. The results will show that incremental feature weighting in EFC in fact helps to reduce curse of dimensionality and therefore guides the evolving fuzzy classifiers to a higher on-line predictive power.

Key words: incremental feature weighting, dynamic dimension reduction, separability criteria, evolving fuzzy classifiers, *FLEXFIS-Class*, single and multi model architecture, on-line classification

Classifier-based analysis of visual inspection: Gender differences in decision-making

Wolfgang Heidl, Stefan Thumfart, Christian Eitzinger WOLFGANG.HEIDL@PROFACTOR.AT
Profactor GmbH, 4407 Steyr-Gleink, AUSTRIA

Edwin Lughofer, Erich Peter Klement EDWIN.LUGHOFER@JKU.AT
Johannes Kepler University, 4020 Linz, AUSTRIA

Abstract

Among manufacturing companies there is a widespread consensus that women are better suited to perform visual quality inspection, having higher endurance and making decisions with better reproducibility. Up to now gender-differences in visual inspection decision making have not been thoroughly investigated. We propose a machine learning approach to model male and female decisions with classifiers and base the analysis of gender-differences on the identified model parameters. A study with 50 male and 50 female subjects on a visual inspection task of stylized die-cast parts revealed significant gender-differences in the miss rate ($p = 0.002$), while differences in overall accuracy are not significant ($p = 0.34$). On a more detailed level, the application of classifier models shows gender differences are most prominent in the judgment of scratch lengths ($p = 0.005$). Our results suggest, that gender-differences in visual inspection are significant and that classifier-based modeling is a promising approach for analysis of these tasks.

1. Introduction

Quality control typically involves the visual inspection of products at the end of a production line. This task is quite often done by women. Their job is to make a quick accept/reject decision and to sort out the bad products. Manufacturing companies often argue that women have more endurance in performing this task and also make decisions with better reproducibility. To our knowledge gender differences in visual inspection decision-making have not been thoroughly investigated.

There is vast literature on sex differences in the behavioral sciences concerning numerous standardized tests on physical strength, spatial orientation, verbal and navigation abilities to name but a few. In the ergonomics and human factor engineering community visual inspection has been extensively studied (Drury & Watson, 2002; Harris & Chaney, 1969). Gender differences have been reported in reaction time changes due to acoustic noise (Gramopadhye & Wilson, 1997), however no gender difference has been found on inspection performance (Lehto & Buck, 2007).

The analysis model for inspection tasks is usually separated into two components, visual search and decision-making (Drury, 1978). In this paper we focus on the latter and investigate the differences between the male and female decision-making processes by taking a machine learning (ML) approach. In the context of ML the problem of separating parts into a good and bad by generalizing from training data is tackled by so called classifiers.

We utilize ML classifiers (Alpaydin, 2004) as a mathematical model of the decision behavior of individual subjects (Figure 1). The goal of model identification, also known as learning, is to generalize from subject responses to specific stimuli to all stimuli stemming from the same random process. Once a ML classifier has been trained that generalizes well, the classifier parameters convey the task-relevant information on subject decision behavior. Further analysis can then be based on these parameters.

Classifiers have recently been successfully applied to complex visual inspection tasks (e.g. (Eitzinger et al.,

This work has been supported by the FEMtech program of The Federal Ministry for Transport, Innovation and Technology under FFG grant No. 318113. It reflects only the authors' views.

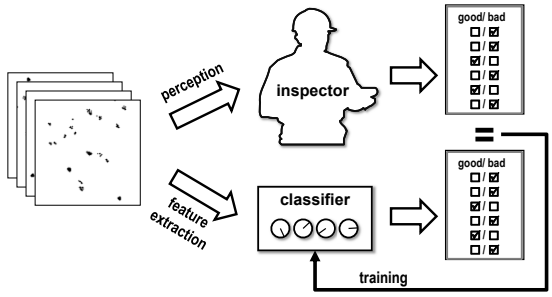

Figure 1. Classifiers modeling human decisions in visual inspection. During training the classier parameters (displayed as tuning knobs) are adjusted to minimize the discrepancy between human and classier decisions.

2009; Lughofer et al., 2009)). However, up to now they are mainly based on considerations of statistics and probability distributions of the features that they classify (Vapnik, 1999; Duda et al., 2000; Hastie et al., 2009). The fact that the decision is originally made by a human is often neglected. Consequently, there has been no investigation of differences in male and female decision-making from the viewpoint of classifiers.

In a real-world inspection scenario when the same set of training samples (images) is shown to different users (with different age, gender, education, nationality etc.), significantly different classifiers and furthermore classification decisions can be expected. Therefore, it is interesting to (empirically) examine these differences among different groups of people. In particular, it would be interesting to verify the claim by manufacturing companies that women are able to make decisions with higher accuracy and better reproducibility.

In this paper we propose a novel design and analysis approach for visual inspection studies according to gender differences in decision-making and classification behavior. We apply this approach to a study with 50 female and 50 male subjects, where we identify significant gender differences concerning miss rate and the judgment of scratch-type faults.

Acknowledgment

The authors would like to thank Daniela Kirchberger who organized recruitment of the subjects and carried out the majority of experiment sessions.

References

Alpaydin, E. (2004). *Introduction to machine learning.* Adaptive Computation and Machine Learning. New York: MIT Press.

Drury, C. G. (1978). Integrating human factors models into statistical quality control. *Human Factors: The Journal of the Human Factors and Ergonomics Society*, *20*, 561–572.

Drury, C. G., & Watson, J. (2002). *Good practices in visual inspection* (Technical Report). Federal Aviation Administration/Office of Aviation Medicine, Washington DC.

Duda, R. O., Hart, P. E., & Stork, D. G. (2000). *Pattern classification.* Wiley-Interscience. 2 edition.

Eitzinger, C., Heidl, W., Lughofer, E., Raiser, S., Smith, J., Tahir, M., Sannen, D., & Van Brussel, H. (2009). Assessment of the influence of adaptive components in trainable surface inspection systems. *Machine Vision and Applications.*

Gramopadhye, A., & Wilson, K. (1997). Noise, feedback training, and visual inspection performance. *International Journal of Industrial Ergonomics*, *20*, 223–230.

Harris, D. H., & Chaney, F. B. (1969). *Human factors in quality assurance.* New York: Wiley.

Hastie, T., Tibshirani, R., & Friedman, J. (2009). *The elements of statistical learning: Data mining, inference, and prediction, second edition (springer series in statistics).* Springer. 2nd ed. 2009. corr. 3rd printing edition.

Lehto, M. R., & Buck, J. (2007). *Introduction to human factors and ergonomics for engineers.* CRC Press. 1 edition.

Lughofer, E., Smith, J., Caleb-Solly, P., Tahir, M., Eitzinger, C., Sannen, D., & Nuttin, M. (2009). On human-machine interaction during on-line image classifier training. *IEEE Transactions on Systems, Man and Cybernetics, part A - Systems and Humans*, *39*, 960–971.

Vapnik, V. N. (1999). *The nature of statistical learning theory.* Statistics for Engineering and Information Science. Springer, Berlin.